Iran J Sci Technol Trans Sci (2018) 42:547–555
https://doi.org/10.1007/s40995-016-0076-x

RESEARCH PAPER

Synthesis of MgO Nanoparticles Using *Artemisia abrotanum* Herba Extract and Their Antioxidant and Photocatalytic Properties

Renata Dobrucka[1]

Received: 6 May 2016 / Accepted: 3 August 2016 / Published online: 2 September 2016

Abstract The synthesis of metal oxide nanoparticles with the use of plant extract is a promising alternative to traditional chemical methods. The aim of this work was to fabricate MgO nanoparticles using the *Artemisia abrotanum* herb water extract. The biologically synthesized MgO nanoparticles were characterized by UV–Visible spectroscopy, Fourier transform infrared spectroscopy (FTIR), X-ray diffraction (XRD), scanning electron microscopy (SEM) with EDS profile and transmission electron microscopy (TEM). XRD studies confirmed that pure monoclinic crystallite structures of MgO nanoparticles were formed. The average size of MgO nanoparticles was found to be 10 nm. EDS profile confirmed the signal characteristic of magnesium and oxygen. FTIR analysis confirmed the presence of active compounds responsible for the stabilization of MgO nanoparticles. The synthesized nanoparticles showed good catalytic activity in the reduction of methyl orange (MO). MgO nanoparticles also exhibit very good antioxidant properties.

Keywords Magnesium oxide nanoparticles · Biosynthesis · Catalytic activity

1 Introduction

Nowadays, researchers have developed exciting new materials in nanosize to progress the unique and tunable properties of the applied materials (Sahoo et al. 2007). Due to their small size, nanoparticles exhibit novel material properties, which are significantly different from those of their bulk counterparts (Bindhu et al. 2016). An important aspect of nanoscience is related to the design of experimental methods for the synthesis of nanoparticles (NPs) of different chemical composition, size, shape and properties (Rai and Yadav 2013). Recently, researchers have tried to find biological methods for the synthesis of nanoparticles that will be the alternative to chemical or physical methods. Biological methods for the production of NPs are considered safe and environmentally friendly; they are also cost-effective and ensure the complete elimination of toxic chemicals (Okitsu et al. 2007). In addition, the synthesis of NPs using biological means, especially plants, is biocompatible, as they secrete functional biomolecules which actively reduce metal ions (Rai and Ingle 2012).

This study presents a biological method for the synthesis of Mg NPs using the extract of *Artemisia abrotanum* herb. Magnesium oxide NPs are highly ionic nanoparticulate metal oxides with extremely high surface areas and unusual crystal morphologies (Ravishankar Rai and Jamuna Bai 2011). Nanoscale MgO possesses unique optical, electronic, magnetic, thermal, mechanical and chemical properties due to its characteristic structures (Ramanujam and Sundrarajan 2014). Magnesium oxide is an important functional metal oxide that has been widely used in various fields, such as catalysis, refractory materials, paints, and superconductors (Salem et al. 2015). In the literature, there are several methods for the synthesis of nano-sized MgO particles, including the sol–gel method, chemical gas phase deposition, laser vaporization, hydrothermal synthesis, and combustion aerosol synthesis (Mirzaei and Davoodnia 2012). Biological methods for the synthesis of MgO NPs with the use of plant materials have not been widely exploited (Sushma et al. 2015). Based on the literature,

✉ Renata Dobrucka
renata.dobrucka@ue.poznan.pl

[1] Department of Industrial Products Quality and Ecology, Faculty of Commodity Science, Poznan University of Economics, al. Niepodległości 10, 61-875 Poznan, Poland

there are some samples of the synthesis of MgO NPs using Clitoria ternatea, neem leaves (Moorthy et al. 2015), Parthenium (Kumar et al. 2015), Brassica oleracea, Punica granatum peels (Sugirtha et al. 2015), citrus lemon (Awwad et al. 2014) or the extract derived from Nephelium lappaceum L peels (Suresh et al. 2014). Therefore, the application of green synthesis in order to obtain MgO NPs is still an unexplored area, which presents numerous research opportunities.

In this work, the synthesis of magnesium oxide was performed using the extract derived from *A. abrotanum* herb. The genus of Artemisia (*Artemisia L.*) includes subshrubs, perennials, plants found mainly in the Holarctic ecozone, on the steppe, on the desert and in the semi-arid areas of Eurasia, Central America and North America. As regards the number of species, this is one of the most numerous genera of the *Asteraceae* family. *A. abrotanum* L. has been used in traditional medicine for treating a variety of disorders, including upper airway diseases (Gruenwald 2000). Due to the fact that *A. abrotanum L.* contains significant amounts of polyphenols, together with an original distribution of polyphenols, flavonoids (aglycones and glycosylates) and hydroxycinnamic derivatives, there is an opportunity for new applications of this herbal extract. So far, the literature has not described the synthesis of MgO NPs using *A. abrotanum* herb extract (Baiceanu et al. 2015). Therefore, the aim of this work was first to obtain and characterize MgO NPs, and then to examine their catalytic activity.

2 Experimental

All reagents used in the present work were purchased from Sigma-Aldrich (Poland). Milli-Q water was used throughout the experiment.

2.1 Synthesis of MgO Nanoparticles

MgO NPs were synthesized using clean, dried and powdered *A. abrotanum* herb. *A. abrotanum* herb was collected from the region of Silesian Plain (Poland). The powdered *A. abrotanum* herb was mixed with double distilled water in the proportion: 2 [% weight] : 98 [% weight]. The mix was kept at 80 °C for 40 min with vigorous magnetic stirring. The obtained solution was filtered through Whatman's No. 1 filter paper. In the next stage, the prepared extract was mixed with Mg $(NO_3)_2$ in the proportion: 90 [% weight]: 10 [% weight] and it was vigorously stirred for 6 h at 90 °C. The prepared solution was set aside for 24 h and kept at 25 °C.

2.2 Characterization of MgO Nanoparticles

The synthesis of MgO NPs using the extract of *A. abrotanum* herba was monitored after precipitate formation using UV–Visible spectrophotometer, Cary E 500, at a wavelength range 250–800 nm. The morphology of MgO NPs was examined by means of scanning electron microscopy (SU3500, Hitachi, with spectral imaging system Thermo Scientific NSS (EDS), the tape of detector (BSE-3D), acceleration voltage (15.0 kV), working distance (11.6 mm), the pressure (in the case of a variable vacuum conditions) (40 Pa). The functional groups attached to the surface of nanoparticles and the other surface chemical residues were detected using FTIR. The characterization involved Fourier transform infrared spectroscopy (FTIR) analysis of the synthesized MgO NPs by Perkin Elmer Spectrum 1000 spectrum in attenuated total reflection mode, and using the spectral range 4000–400 cm^{-1} with the resolution of 4 cm^{-1}. The size and structure of MgO NPs were characterized using a transmission electron microscope JEOL JEM 1200 EXII, operating at 200 kV. X-ray diffraction studies of the MgO NPs were carried out using a BRUKER D8 ADVANCE brand *−2* configuration (generator-detector) X-ray tube copper $S = 1.54$ A and LYNXEYE PDS detector. The size of particles was estimated on the basis of Scherrer's formula.

2.3 Catalytic Properties of MgO Nanoparticles

The catalytic activity of MgO NPs synthesized using the extract of *A. abrotanum* herb was evaluated using UV–Vis spectrophotometer, Cary E 500, to monitor the absorbance peaks. The absorbance was measured in the range 350–800 nm at room temperature. The proper concentration of methyl orange (1×10^{-4}M) was chosen on the basis of the literature review. In the first reaction mixture, the aqueous solution of methyl orange (1×10^{-4}M) was monitored by measuring the intensity of absorbance. In the second reaction mixture, 4 ml of methyl orange (MO), 0.5 ml of *A. abrotanum* water extract and 3 ml of Milli Q water were analyzed. The study of decomposition of methyl orange (MO) used the same amounts of methyl orange and *A. abrotanum* water extract, i.e. 4 ml of MO and 0.5 ml of *A. abrotanum* water extract. For the variant MO I, 0.5 ml of the prepared solution of MgO NPs and 2.5 ml of Milli Q water were used. For other variants, i.e. from variant MO II to variant MO V, the amounts of the prepared solution of MgO NPs were successively increased by 0.5 ml, and the amounts of Milli Q water were successively decreased by 0.5 ml. All variants were exposed to sunlight for 120 min.

2.4 Antioxidant Activity

In this work, the antioxidant activity was determined by assessing the ability of MgO NPs synthesized using the extract of *A. abrotanum* to neutralize the DPPH (2,2-diphenyl-1-picrylhydrazyl) radical, which was reflected by the reduction of the absorbance of the DPPH methanol solution during the reaction with the tested solution of MgO NPs. There were numerous dilutions prepared in the range 0.01–5 μg/ml. Changes in the absorbance intensity were measured using the spectrophotometer, Cary E 500. To the test tubes (protected from light) were added 0.1 ml of the tested solution and 0.7 ml of the DPPH reagent at the concentration of 0.1 mM. The DPPH reagent was prepared 24 h in advance (protected from light). After 30 min of shaking the solutions in test tubes, the absorbance was read, at the wavelength $\lambda = 515$ nm. Water (0.1 ml) and methanol (0.7 ml) were used as reference. Before the measurement of the absorbance of samples, the absorbance of DPPH solution was measured. The measurement was made by measuring the absorbance of 0.1 ml of deionized water and 0.7 ml of DPPH solution. The ability to reduce free DPPH radicals was calculated based on the formula:

$$\mathrm{Aa} = (\mathrm{Ao} - \mathrm{Ai}/\mathrm{Ao}) \times 100\,\%,$$

where Aa means antioxidant activity [%], Ai means average absorbance of the tested solution, and Ao means average absorbance of the DPPH solution.

2.5 Statistical Analysis

The results presented in the work constitute the arithmetic mean of five measurements carried out in parallel. The mean and the standard deviations were calculated using the Statistica 8.0 computer program.

3 Results and Discussion

3.1 UV–Visible Absorption

UV–Vis absorption spectroscopy is the most widely used method for characterizing the optical properties and electronic structure of nanoparticles, as the absorption bands are relatedto the diameter and aspect ratio of metal nanoparticles (Philip 2008). In this study, the prepared MgO NPs were confirmed by UV–Vis spectroscopy. According to Feldheim and Foss (2002), light wavelengths in the 300–800 nm are used for characterizing various metal nanoparticles in the size range 2–100 nm. This work used the range 250–800 nm to identify MgO NPs. The prepared solution was set aside for 24 h and kept at 25 °C. Figure 1 presents the UV–Visible spectra of MgO NPs synthesized using the extract of *A. abrotanum* herb after 24 h. The absorption spectra of the reaction media with absorbance at 300 nm confirmed the presence of MgO NPs. This proves the reduction of Mg $(NO_3)_2$ and the emergence of MgO. The presence of MgO was confirmed by conducting such studies as SEM with EDS profiles, TEM, FTIR and DLS. Figure 2 presents the synthesis scheme of MgO NPs synthesized using of *A. abrotanum* herba extract.

3.2 FTIR Analysis

Fourier transform infrared spectroscopy (FTIR) was used to identify the possible biomolecules which are responsible for the reduction and capping of MgO NPs. Figure 3 presents the FTIR spectra of MgO NPs synthesized using the *A. abrotanum* herb extract. The spectra show bands at 3308, 2139, 1635, 1346, 419 and 407 cm^{-1}. The strong infrared band near 3308 cm^{-1} was observed for the O–H bond vibrations of hydroxy group. The most intense band at 1635 cm^{-1} represents vibrations C=O, typical for the structure of flavonoids which can be found in the *A. abrotanum* herb extract. The peak which appeared at 2139 cm^{-1} may indicate the presence of alkynes group. The absorption band at 1346 cm^{-1} is related to C–H bending vibrations of aromatic tertiary amine group. The peaks observed at 419 cm^{-1} and 407 cm^{-1} indicate the presence of MgO NPs. FTIR spectrum confirmed the presence of bioactive compounds in *A. abrotanum* herb. These bioactive compounds were presumed to act as

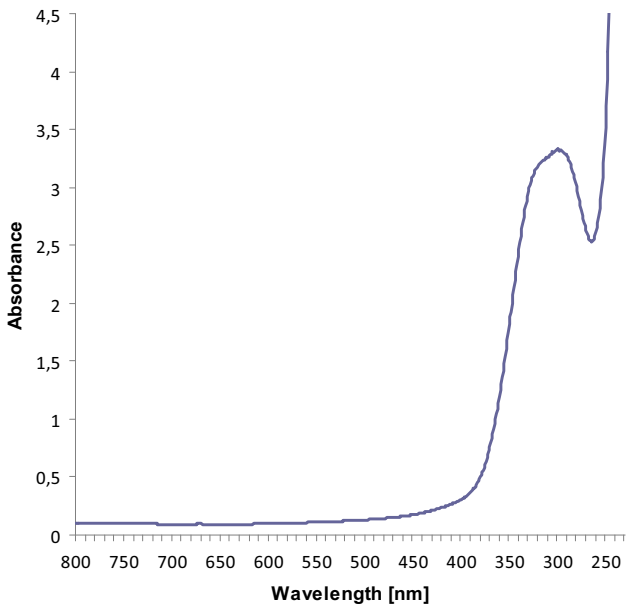

Fig. 1 Absorption spectra of MgO nanoparticles synthesized using of *A. abrotanum* herba extract

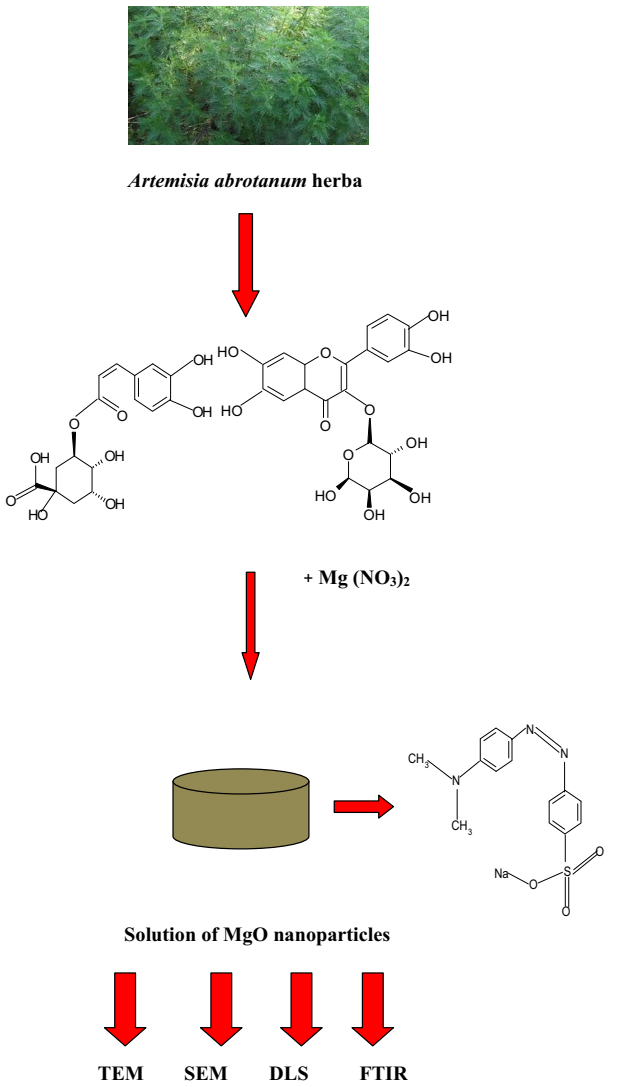

Fig. 2 The scheme synthesis of MgO nanoparticles synthesized using *A. abrotanum* herba extract

reducing and capping agents for MgO NPs. According to the literature, the essential oil from *A. abrotanum* contains 68 identified compounds (Kowalski et al. 2007). The main constituents of the oil are: piperitone, davanone, linanool, 1,8-cineole, silphiperfol-5-en-3-ol A and germacrene D. Furthermore, in the herbal extract of *A. abrotanum* L., several phenolic acids were identified: gentisic, caffeic, chlorogenic, *p* coumaric, ferulic and sinapic acid, both before and after acid hydrolysis. Moreover, *A. abrotanum* contains several flavonoid aglycones: quercetrol, luteolin, apigenin, and the most abundant flavonoids: hyperoside, rutin, quercetol, patuletin, luteolin, kaempferol. As it is known, phenolic compounds have good antioxidant properties; they inhibit the production of reactive oxygen species (ROS), and thus constitute a protection against oxidative stress. In numerous scientific studies on the antioxidant properties of phenolic acids, researchers have proven the correlation between these properties and the chemical structure. More specifically, the antioxidant properties are related to the number of hydroxy groups in the particle, as well as the level of their esterification. In compounds with one hydroxy group, the antioxidant activity is additionally increased by the presence of one or two methoxy groups in the ring. The introduction of a group with electron donors, alkyl or methoxy, in the *ortho*-position, reinforces the stability of the antioxidant properties of phenolic acids. (Cuvelier et al. 1996; Shahidi and Wanasundara 1992). The extract of *A. abrotanum* includes chlorogenic acid, which demonstrates high antioxidant activity. The presence of chlorogenic acid and these biologically active compounds is crucial for the reduction and stabilization of MgO NPs. Figure 4 presents the structure of the selected phenolic acids (chlorogenic and caffeic acid) and flavonoids (hyperoside, kaempferol).

3.3 XRD Analysis

The XRD techniques are widely used to determine the size of particles and the structure of nanoparticles. Figure 5 shows the X-ray diffraction profile of MgO NPs synthesized using the *A. abrotanum* herb extract. The size of MgO NPs was obtained by Debye–Scherrer's formula:

$$D = K\lambda/(\beta\cos\theta)$$

where D is the crystal size; λ is the wavelength of the X-ray radiation ($\lambda = 0.15406$ nm) for CuKα; K is usually taken as 0.9; and β is the line width at half-maximum height.

MgO NPs show peaks corresponding to the planes at $2\theta = 39.60°$ (111), $2\theta = 42.90°$ (200), $2\theta = 62.86°$ (202), $2\theta = 74.62°$ (311), $2\theta = 78.60°$ (222). The XRD spectrum suggests that MgO NPs synthesized using the *A. abrotanum* herb extract were crystalline. The crystal sizes calculated using Scherrer's formula were about 10 nm.

3.4 SEM and EDS Profile

Figures 6 present the scanning electron microscopy (SEM) images of the MgO NPs synthesized using the *A. abrotanum* herb extract where the scale bar is (A) 5 µm, (B) 10 µm, (C) 20 µm and (D) 30 µm. Figure 6 shows that the size of single MgO NPs was about 10 nm. Furthermore, the MgO NPs were well dispersed. Locally, the synthesized MgO NPs were agglomerated and formed larger clusters. Figure 7 presents the SEM images of the MgO nanoparticles synthesized using the *A. abrotanum* herb extract where (A) the scale bar is 25 µm and (C) the scale bar is 10 µm with EDS profiles. Further analysis of the MgO NPs by EDS profile confirmed the signal characteristic of

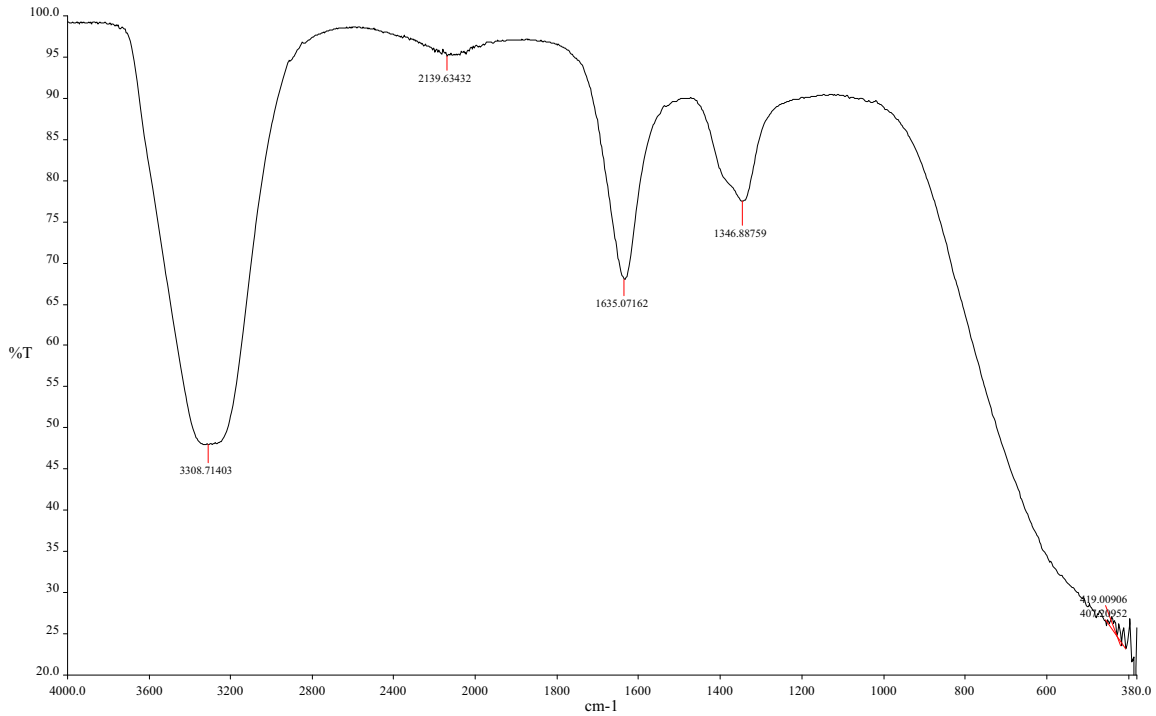

Fig. 3 FTIR spectra of MgO nanoparticles synthesized using *A. abrotanum* herba extract

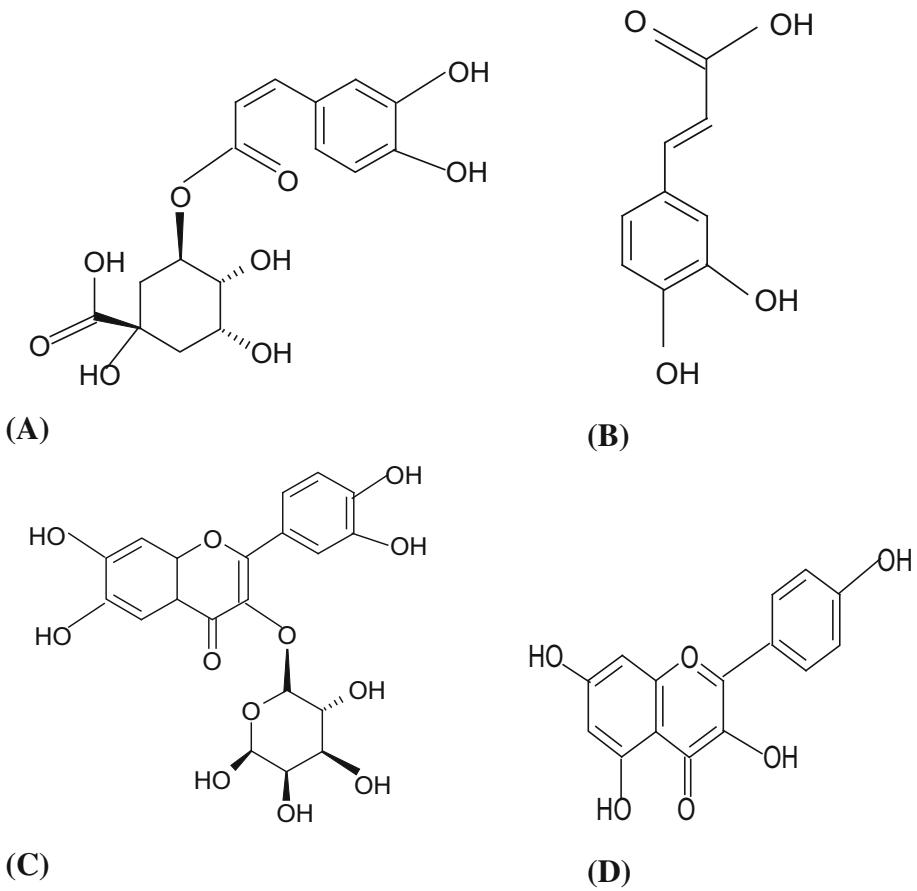

Fig. 4 The structure of selected phenolic acids: **a** chlorogenic, **b** caffeic acid and flavonoids, **c** hyperoside, **d** kaempferol

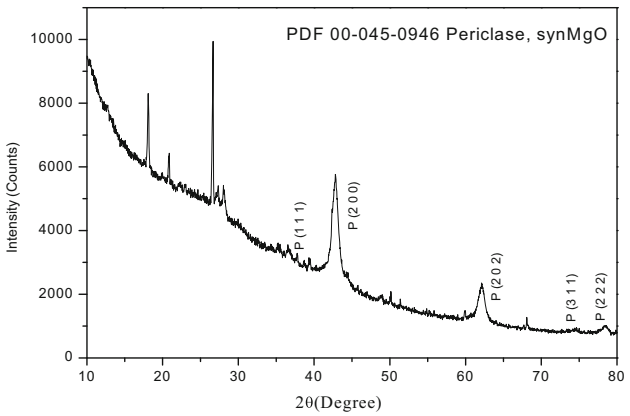

Fig. 5 XRD patterns of synthesized MgO nanoparticles using *A. abrotanum* herba extract

magnesium and oxygen. EDS profile is the additional evidence of the formation of pure MgO nanoparticles. Figure 7b, d presents peaks between 0.5 and 1.5 kV, which indicate the presence of MgO NPs. Figure 7 (B) shows the magnesium content at the level of 25.4 %, and the oxygen content at the level of 47.6 %. The quantities of the remaining elements are as follows: C (23.7 %), Al (0.7 %), Si (0.3 %), P (0.1 %), K (1.0 %) and Ca (0.5 %). Figure 7 (D) shows the magnesium content at the level of 13.9 %, and the oxygen content at the level of 39.4 %. The quantities of the remaining elements are as follows: C (43.8 %), Al (1.4 %), Si (0.3 %), K (0.8 %) and Ca (0.5 %).

The size, shape, and morphologies of the synthesized MgO nanoparticles were examined using transmission electron microscopy (TEM).

3.5 TEM Analysis

The size of the synthesized MgO NPs was characterized by using transmission electron microscopy (TEM). As it is known, TEM is an extremely useful technique to obtain the direct information concerning particle size distribution, mean particle size and the shape of nanoparticles. Transmission electron microscopy has a 1000 times higher resolution than does scanning electron microscopy (Eppler et al. 2000). In this study, it was decided to use both methods in order to measure the size of nanoparticles. The TEM image (Fig. 8 A magnification 50,000× and Figure B magnification 100,000×) confirmed that the size of the synthesized MgO NPs was less than 10 nm. Moreover, the transmission electron microscopy image presents the spherical structure of the synthesized MgO NPs.

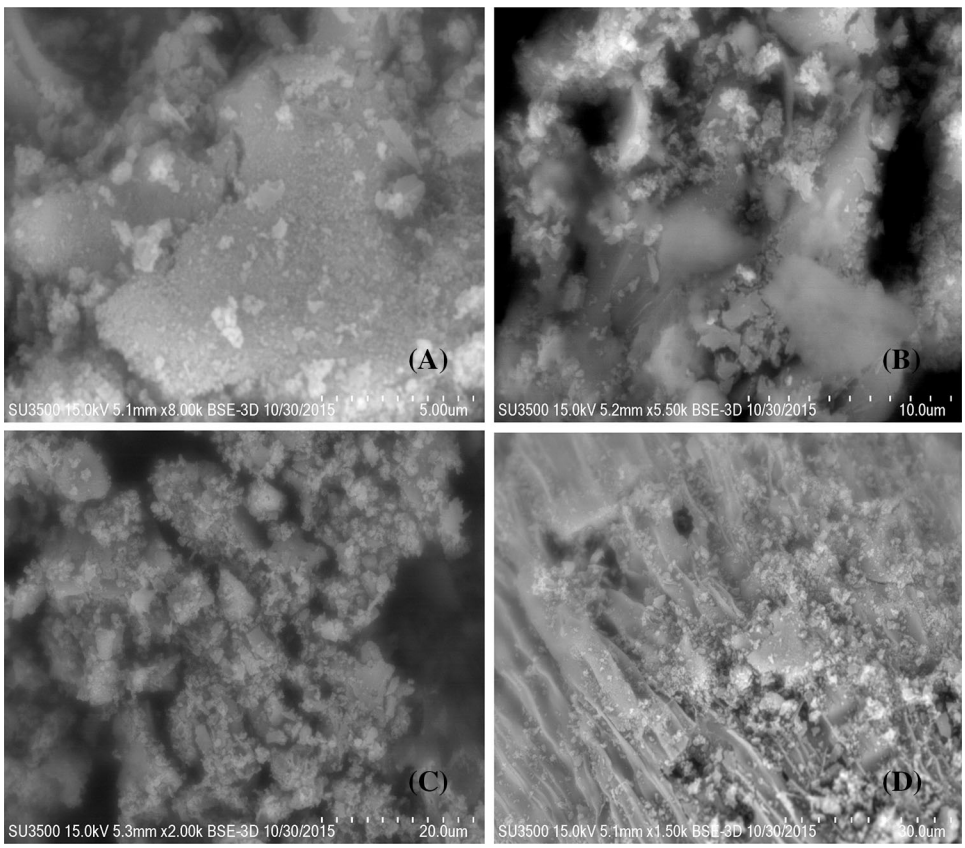

Fig. 6 SEM images of the synthesized MgO nanoparticles synthesized using *A. abrotanum* herba extract where the *scale bar* is **a** 5 μm, **b** 10 μm, **c** 20 μm and **d** 30 μm

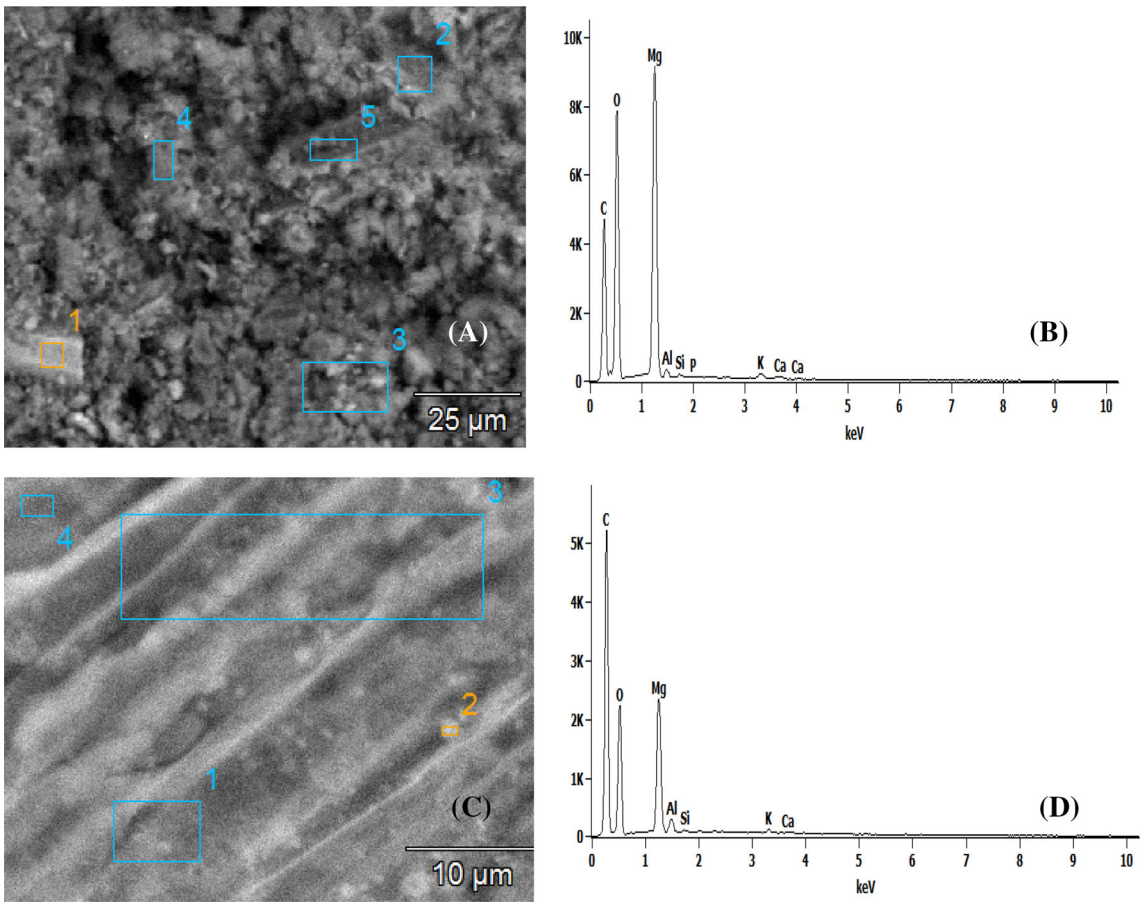

Fig. 7 SEM images of the MgO nanoparticles where **a** the *scale bar* is 25 µm and **c** the *scale bar* is 10 µm and EDS profiles (**b**, **d**)

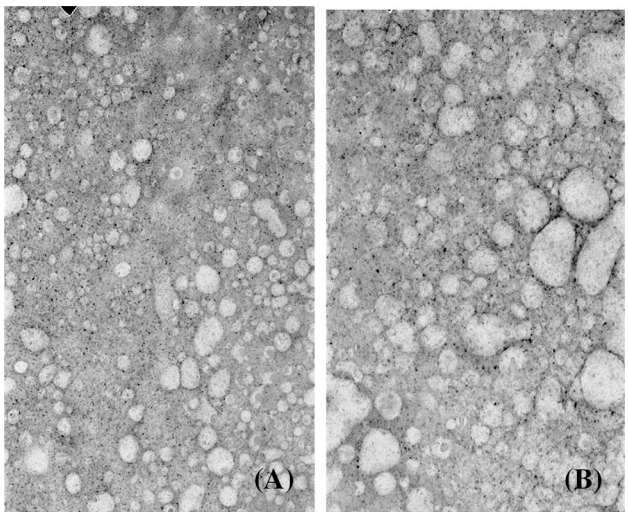

Fig. 8 TEM image of the synthesized MgO nanoparticles **a** magnification 50,000× and **b** magnification 100,000×

3.6 Catalytic Activity of MgO Nanoparticles

Organic dyes are widely used in many industries. Methyl orange (MO) is a dye which is widely applied in the chemical, textile and paper industries. As the excessive use of organic dyes leads to environmental pollution, the control of industrial effluents is an indispensable job, which helps in the creation of harmless and clean environment (Ganapuram et al. 2015). Therefore, the search for a simple method for the efficient degradation of dyes has gained greater significance. One of such solutions may be the application of metal oxide nanoparticles, which show enhanced catalytic activity in the degradation of organic dyes (Ashokkumar et al. 2014). In this study, MgO NPs were used as a catalyst for the remediation of methyl orange (MO). Figure 9 shows the reduction of methyl orange (MO) in the absence of synthesized MgO NPs for a time period of 120 min. The study used variants from MO I to MO V; in each variant, the amount of the prepared solution of MgO NPs was successively increased by 0.5 ml, while the amount of water was successively decreased by 0.5 ml. The maximum absorbance wavelength of methyl orange was recorded at 464 nm. The diagram explicitly shows that the degradation of MO advances due to the increasing amount of the prepared solution of MgO NPs. This study confirms the catalytic properties of green synthesized MgO NPs. These results

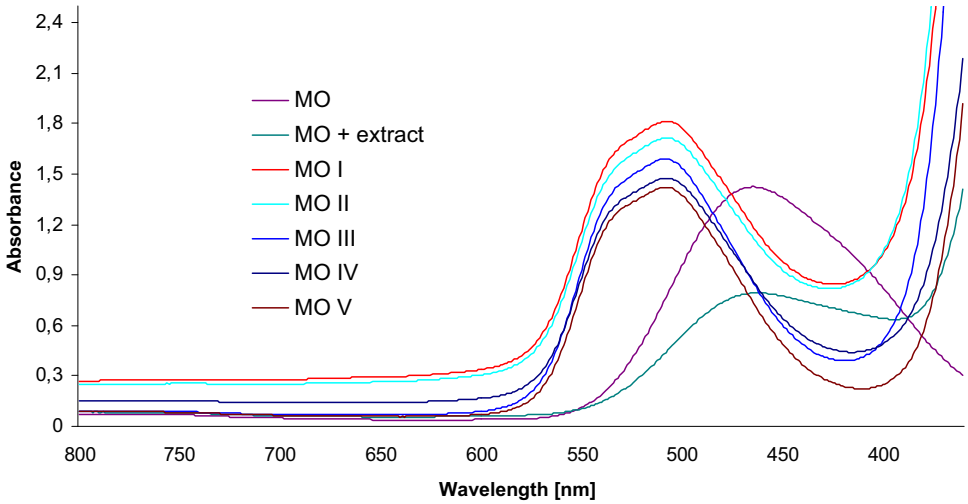

Fig. 9 Absorption spectra of methyl orange reduction by MgO nanoparticles synthesized using *A. abrotanum* herba extract

may be complementary to the studies conducted by Gupta et al. (2011), who synthesized gold, silver and platinum nanoparticles using tannic acid as the reducing agent. The prepared metal nanoparticles were used for the catalytic degradation of methyl orange in the presence of $NaBH_4$. The international literature describes only few studies related to the catalytic properties of the MgO NPs obtained as a result of biological synthesis. One of such studies is presented by Mirzaei and Davoodnia (2012), who used microwave-assisted sol–gel method for the preparation of nano-sized MgO particles. The synthesized MgO NPs exhibited high catalytic activity and gave the desired products in good to high yields. This work presents the catalytic activity of biologically synthesized MgO NPs, which may be applied in the degradation of organic dyes.

3.7 Antioxidant Activity of MgO Nanoparticles

The antioxidant activity of MgO NPs synthesized using the *A. abrotanum* herb extract was determined by means of the test using the DPPH radical. In the DPPH method, antioxidants present in the tested sample reduce the stable nitrogen radical 2,2-diphenyl-1-picrylhydrazyl (DPPH), causing the decrease in absorbance measured at the wavelength of 515 nm. Substances that can donate an oxygen atom create the reduced form of DPPH; in consequence, the solution loses its violet color. In this work, the solution of the active radical was purple, which proved that the previously unpaired electron became paired. The level of color change of the DPPH solution after adding the solution with antioxidants shows the free radical scavenging properties of the antioxidants. This study also investigated the antioxidant activity of the only extract of *A. abrotanum* herb. There were five separate measurements conducted, which were repeated five times. In this work, the antioxidant properties of MgO NPs synthesized using the *A. abrotanum* herb extract were determined by calculating the IC50 parameter. This parameter determines the ability to scavenge free radicals. The higher the IC50 parameter, the more reactive the antioxidant. For MgO NPs, the mean value of the parameter, based on five measurements, was 4.73 μg/ml. For comparison, for the extract of *A. abrotanum* herb, the mean value of the parameter, based on five measurements, was 6.28 μg/ml. The obtained result indicated the high antioxidant activity of the obtained MgO NPs. The presence of MgO nanoparticles led to a considerable improvement of the antioxidant activity of the *A. abrotanum* herb extract. Table 1 shows the results obtained for the antioxidant activity of MgO NPs synthesized using the *A. abrotanum* herb extract, as well as of the *A. abrotanum* herb extract itself.

4 Conclusion

Nanoscience and technology have become the new hot topics in material science. Nanostructured oxide materials have been studied extensively because of their large surface areas, unusual adsorptive properties, surface defects and fast diffusivities. Recently researchers have discovered the possibilities of preparing nanomaterials in an aqueous medium with the help of stabilizing, capping or hydrolytic

Table 1 The results of antioxidant activity of MgO NPs and the extract of *A. abrotanum* herb

Product	IC_{50} (μg/ml)	SD
MgO NPs	4.73	0.10
A. abrotanum herb extract	6.28	0.01

IC50 inhibitory concentration 50 %, *SD* standard deviation

agents. This study also examined the roles of the water extract of *A. abrotanum* herb in the formation and stabilization of MgO NPs. The synthesized nanostructures have been characterized by UV–Vis, FTIR, XRD, TEM and SEM with EDS profile. The obtained MgO NPs, sized about 10 nm, have shown the catalytic activity in the photodegradation of MO. To sum up, this study presents the ecological method for preparing nanoparticles without the need of using harmful chemical substances. The obtained MgO NPs may have potential applications due to their good catalytic activity. MgO NPs also showed strong antioxidant properties.

Acknowledgments Research on the synthesis of MgO nanoparticles using *A. abrotanum* herba extracts and their catalytic activity has been financed from the grant for young researchers in 2015 by the Ministry of Science and Higher Education.

References

Ashokkumar S, Ravi S, Kathiravan V, Velmurugan S (2014) Synthesis, characterization and catalytic activity of silver nanoparticles using Tribulus terrestris leaf extract, Spectrochim. Acta Part A Mol Biomol Spectrosc 121:88–93

Awwad AM, Ahmad AL (2014) Biosynthesis, characterization, and optical properties of magnesium hydroxide and oxide nanoflakes using *Citrus limon* leaf extract. Arab J Phys Chem 1(2):66

Baiceanu E, Vlase L, Baiceanu A, Nanes M, Rusu D, Crisan G (2015) New polyphenols identified in artemisiae abrotani herba extract. Molecules 20:11063–11075

Bindhu MR, Umadevi M, Micheal MK, Arasu MV, Al-Dhabi NA (2016) Structural, morphological and optical properties of MgO nanoparticles for antibacterial applications. Mater Lett 166:19–22

Cuvelier ME, Richard H, Berset C (1996) Antioxidative activity and phenolic composition of pilot-plant and commercial extracts of sage and rosemary. J Am Oil Chem Soc 73(5):645–652

Eppler AS, Zhu J, Anderson EA, Somorjai GA (2000) Model catalysts fabricated by electron beam lithography: AFM and TPD surface studies and hydrogenation/dehydrogenation of cyclohexene + H2 on a Pt nanoparticle array supported by silica. Top Catal 13:33–41

Feldheim DL,. Foss CA (eds) (2002) Metal nanoparticles: synthesis, characterization and applications (Marcel Dekker Inc.)

Gruenwald J (2000) PDR for herbal medicines. Montvale

Gupta N, Singh HP, Kumar Dharma R (2011) Metal nanoparticles with high catalytic activity in degradation of methyl orange: an electron relay effect. J Mol Catal A: Chem 335:248–252

Kowalski R, Wawrzykowski J, Zawiślak G (2007) Analysis of essential oils and extracts from *Artemisia abrotanum* L. and *Artemisia dracunculus L.* Herba Pol 53(3):246–254

Kumar D, Reddy Yadav LS, Lingaraju K, Manjunath K, Suresh D, Prasad D, Nagabhushana H, Sharma SC, Raja Naika H, Chikkahanumantharayappa, Nagaraju G (2015) Combustion synthesis of MgO nanoparticles using plant extract: structural characterization and photoluminescence studies. AIP Conf Proc 1665:050145

Mirzaei H, Davoodnia A (2012) Microwave assisted sol-gel synthesis of MgO nanoparticles and their catalytic activity in the synthesis of hantzsch 1, 4-dihydropyridines. Chin J Catal 33:1502–1507

Moorthy SK, Ashok CH, Venkateswara Rao K, Viswanathan C (2015) Synthesis and characterization of MgO nanoparticles by Neem leaves through green method. Mater Today Proc 2:4360–4368

Okitsu K, Mizukoshi Y, Yamamoto TA, Maeda Y, Nagata Y (2007) Sonochemical synthesis of gold nanoparticles on chitosa. Lett Mater 61(16):3429–3431

Philip D (2008) Synthesis and spectroscopic characterization of gold nanoparticles. Spectrochimica Acta Part A 71:80–85

Rai M, Ingle A (2012) Role of nanotechnology in agriculture with special reference to management of insect pests 94(2):287–293

Rai M, Yadav A (2013) Plants as potential synthesizer of precious metal nanoparticles: progress and prospects. IET Nanobiotechnol 3:117–124

Ramanujam K, Sundrarajan M (2014) Antibacterial effects of biosynthesized MgO nanoparticles using ethanolic fruit extract of Emblica officinalis. J Photochem Photobiol, B 141:296–300

Ravishankar RV, Jamuna BA (2011) Nanoparticles and their potential application as antimicrobials. Science against microbial pathogens. Communicating current research and technological advances. A. Méndez-Vilas (Ed.), pp 197–209

Reddy Ganapuram B, Alle M, Dadigala R, Dasari A, Maragoni V, Guttena V (2015) Catalytic reduction of methylene blue and Congo red dyes using green synthesized gold nanoparticles capped by salmalia malabarica gum. Int Nano Lett 5:215–222

Sahoo SK, Parveen S, Panda JJ (2007) The present and future of nanotechnology in human health care. Nanomed NBM 3(1):20–31

Salem JK, El-Nahhal IM, Hammad TM, Kuhn S, Sharekh SA, El-Askalani M, Hempelmann R (2015) Optical and fluorescence properties of MgO nanoparticles in micellar solution of hydroxyethyl laurdimonium chloride. Chem Phys Lett 636:26–30

Shahidi F, Wanasundara JPD (1992) Phenolic antioxidant. Crit Rev Food Sci Nutr 32:67–103

Sugirtha P, Divya R, Yedhukrishnan R, Suganthi KS, Anusha N, Ponnusami V, Rajan KS (2015) Green synthesis of magnesium oxide nanoparticles using brassica oleracea and punica granatum peels and their anticancer and photocatalytic activity. Asian J Chem 27(7):2513–2517

Suresh J, Yuvakkumar R, Sundrarajan M, Hong SI (2014) Green synthesis of magnesium oxide nanoparticles. Adv Mater Res 952:141–144

Sushma NJ, Prathyusha D, Swathi G, Madhavi T, Deva Prasad Raju B, Mallikarjuna K, Hak-Sung Kim (2015) Facile approach to synthesize magnesium oxide nanoparticles by using Clitoria ternatea—characterization and in vitro antioxidant studies. Appl Nanosci 1–8